Journal Name

ARTICLE TYPE

Cite this: DOI: 10.1039/xxxxxxxxxx

Methanol Dimer Formation Drastically Enhances Hydrogen Abstraction from Methanol by OH at Low Temperature†

Willem Siebrand,[a], Zorka Smedarchina,[a] Emilio Martínez-Núñez,*[b] and Antonio Fernández-Ramos*[b]

Received Date
Accepted Date

DOI: 10.1039/xxxxxxxxxx

www.rsc.org/journalname

The kinetics of the reaction of methanol with hydroxyl radicals is revisited in light of reported new kinetic data, measured in cold expansion beams. The rate constants exhibit an approximately 10^2-fold increase when the temperature decreases from 200 to 50 K, a result that cannot be fully explained by tunneling, as we confirm by new calculations. These calculations also show that methanol dimers are much more reactive to hydroxyl than monomers and imply that a dimer concentration of about 30 % of the equilibrium concentration can account quantitatively for the observed rates. The assumed presence of dimers is supported by the observation of cluster formation in these and other cold beams of molecules subject to hydrogen bonding. The calculations imply an important caveat with respect to the use of cold expansion beams for the study of interstellar chemistry.

Introduction

The reaction of methanol with hydroxyl radicals, producing methoxy and hydroxymethyl radicals has received much attention because of its importance in combustion chemistry.[1–3] In addition, Shannon et al.[4] (hereafter SBGH) have recently suggested that it may also play a part in interstellar chemistry as a possible source of recently detected methoxy radicals,[5–7] a suggestion based on their remarkable observation using a Laval nozzle that at low temperatures the reaction proceeds at a rate that is up to two orders of magnitude larger than at room temperature. A more recent report by the same group[8] added more data points (including flow tube experiments above 120 K) and a more detailed discussion of the reaction kinetics, but without changing the interpretation of SBGH, who, on the basis of potentials calculated by Xu and Lin,[1] proposed a two-step reaction mechanism:

$$CH_3OH + OH \overset{k_{1,M}}{\rightarrow} C \qquad (R1)$$

$$C \overset{k_{-1,M}}{\rightarrow} CH_3OH + OH \qquad (R\text{-}1)$$

namely formation of a metastable complex, C, between the two reactants followed by hydrogen tunneling through a barrier:

$$C \overset{k_{2a,M}}{\rightarrow} CH_2OH + H_2O \qquad (R2a)$$

$$C \overset{k_{2b,M}}{\rightarrow} CH_3O + H_2O \qquad (R2b)$$

In this picture a high rate of reaction will result when the lifetime of the complex is long on the time scale of the tunneling rate, since then the reaction rate would equal the rate of complex formation (the capture rate). Since the lifetime of the complex is governed by the sum of the dissociation and the tunneling rates, the argument requires a low dissociation rate at low temperature. This is a critical requirement since the association step yields a hot complex, which will have a short lifetime unless it is effectively cooled. SBGH addressed this problem, but their calculated rates at low temperatures significantly underestimate the observed rates (by an order of magnitude) and also the temperature dependence of the rates. The discrepancy is large enough to call the interstellar application into question.

It is the purpose of this article to investigate whether this discrepancy can be removed by recalculating the relevant potentials and the reaction dynamics, or requires a new interpretation of the experiments. The experimental results indicate that, as the temperature is lowered from 200 to 50 K, the rate constants increase by roughly two orders of magnitude. This may indicate

[a] National Research Council of Canada, Ottawa, Ontario K1A 0R6, Canada
[b] Centro de Investigación en Química Biolóxica e Materiais Moleculares (CIQUS) e Departamento de Química Física, Universidade de Santiago de Compostela, 15782 Santiago de Compostela, Spain
* Electronic mail: emilio.nunez@usc.es, qf.ramos@usc.es

† Electronic Supplementary Information (ESI) available: [It contains details on the MPWB1K/6-31+G(d,p) calculations including geometries, absolute energies and frequencies of the stationary points. It also includes the equilibrium constants for dimer formation, the SCT tunneling probabilities and details on the dynamics calculations: fitting of the $CH_3OH + OH \rightarrow CH_3OH\cdots OH$ potential energy surface, construction of the $(CH_3OH)_2 + OH \rightarrow CH_3OH\cdots OH + CH_3OH$, evaluation of the survival probabilities and internal energy content of the nascent complexes, three representative movies of the dimer mechanism, calculation of the total thermal rate constants and abundance of methoxy radicals. A discussion on the dependence of the pseudo-first order rates on methanol concentration is also included]. See DOI: 10.1039/b000000x/

that tunneling is faster than redissociation back to reactants. It may also indicate that the overall rate k_M approaches the association rate constant $k_{1,M}$, where every complex formed will react. While the observed low-temperature results allow both interpretations, the low value of $k_{-1,M}$ required for $k_{2,M} > k_{-1,M}$ to be true, is incompatible with the observed pressure independence of the low-temperature rate, since the lack of a significant pressure effect implies that the complex retains (most of) its internal energy and thus its high dissociation rate during the reaction. This is the apparent reason why the low-temperature rates calculated by SBGH are too small by an order of magnitude.

In the present article, we review these calculations and also explore another mechanism based on the tendency of molecules with hydroxyl groups to form clusters, in particular dimers.

Methods

We have carried out new electronic structure calculations at the MPWB1K level with the 6-31+G(d,p) basis set.[9] This DFT method is specially recommended for thermochemistry and thermochemical kinetics,[10,11] and together with canonical variational transition state theory with small-curvature tunneling corrections (CVT/SCT) it has been shown to perform well for hydrogen shift reactions at or below room temperature.[12,13] Additionally, we have performed specific tests for the reaction under study, which confirm the adequacy of the MPWB1K/6-31+G(d,p) method in this case. For a more detailed discussion we refer to the Supporting Information (SI).

For the barrierless R1 reaction we started with the reactants at a distance of about 12 Å and followed the gradient along the minimum energy path (MEP) using a stepsize of 0.01 Bohr and performing Hessian calculations every 0.1 Bohr. The normal-mode frequencies along the path were scaled by the recommended factor of 0.964.[14]. For reactions R2a and R2b the MEP was also calculated, and this information was used to evaluate quantum effects by the small-curvature multidimensional tunneling (SCT) approximation.[15,16] Under the conditions of the experiment, variational transition state theory cannot be applied because reaction R1 leads to a complex which is not thermalized and, therefore, R-1 cannot be obtained from the equilibrium constant. In fact $k_{-1,M}$ will be much higher than the rate constant obtained assuming equilibrium. In other words, the internal energy distribution of the molecules of the complex will be very far from a thermalized Boltzmann distribution and therefore we proceed similarly to SBGH: firstly we calculate the thermal rate constant of association $k_{1,M}(T)$, and secondly, we obtain the microcanonical rate constants $k^T_{1,M}(E)$ using an inverse Laplace transform (ILT) method,[17–19]

$$k^T_{1,M}(E) = k_{1,M}(T) P^T_M(E) \quad (1)$$

where $P^T_M(E)$ is the internal energy distribution function at temperature T. The thermal association rate constants $k_{1,M}(T)$ were obtained by building an analytical potential energy surface based on the MPWB1K/6-31G(d,p) electronic structure calculations and using quasi-classical trajectories (QCT). This potential energy surface was fitted to about fourteen hundred single-point MPWB1K/6-31G(d,p) calculations. The dissociation microcanonical rate constants $k_{-1}(E)$ were calculated using variational Rice-Ramsperger-Kassel-Marcus (RRKM) theory and all the modes were treated as harmonic oscillators except the ones corresponding to the two lowest vibrational frequencies in the reactant (C) and variational transition state, which are associated to the OH motion with respect to the methanol molecule. These two harmonic frequencies were replaced by a hindered hard-sphere two-dimensional rotor.[20] In particular, since the reactant complex rotors are more sterically-hindered than those of the variational transition state, the effective rotational constant of the reactant complex was chosen to be 1.6 times larger than that of the transition state to obtain the same rate constant as SBGH at $T = 200$ K. For the tunneling rates associated with reactions R2a and R2b, RRKM theory was employed together with the tunneling probabilities obtained from the SCT approximation. Additionally, pressure effects were taken into account by including collisional energy transfer (CET) rates using an exponential down model with the same parameters as SBGH. From these results, one can then calculate the total thermal rate constant $k_M(T)$ using the master equation. In this work we solve the master equation using kinetic Monte-Carlo (KMC) simulations.[21]

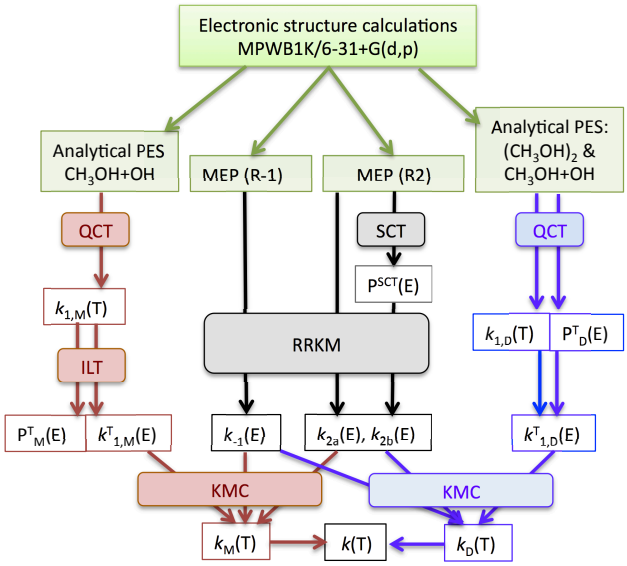

Fig. 1 Flowchart showing the different methodologies used to obtain the individual and overall thermal rate constants

The various methods used to calculate the rates are schematically displayed in Figure 1. The left side outlines the steps taken to obtain the $k_M(T)$ thermal rate constant. Details on the calculations and on the parametrization of the potential energy surface are given in the SI. During the KMC simulations it is possible to monitor the concentration of the different species as a function of time. In fact, KMC can be regarded as a computational kinetic experiment and $k_M(T)$ was obtained in the same manner as the experimental values, i.e., from the decay of the OH radicals.

For the calculation of the total hydrogen abstraction reaction starting from the methanol dimer we have followed a similar procedure as for the monomer (see Figure 1). The microcanonical rate constants $k_{-1}(E)$, $k_{2a}(E)$ and $k_{2b}(E)$ which are the same as

before, are used to calculate the total thermal rate constant $k_D(T)$ from KMC with different association rates $k_{1,D}(T)$ and internal energy distributions of the complex.

The association rates were obtained by performing QCT calculations on a linked potential energy surface obtained from the methanol M + OH potential energy surface plus that of the methanol dimer obtained from Ref. 22 (details are given in the SI).

The electronic structure calculations were performed with Gaussian09.[23] The dynamics QCT calculations were performed with VENUS.[24] The SCT tunneling probabilities were obtained with PolyRate 9.7.[25] RRKM and KMC rate constants were calculated with programs from our research group.

Results and Discussion

Methanol monomer mechanism

Relative energies of the stationary points are given in Figure 2. The geometry of the complex is similar to the one obtained by Xu and Lin,[1] with the hydrogen of the OH molecule pointing towards the oxygen atom of methanol, although the complex obtained at the MPWB1K level is 0.7 kcal/mol more stable then the one reported in Ref. 1. Recently, this complex has been detected using mass spectrometry and infrared spectroscopy.[26]

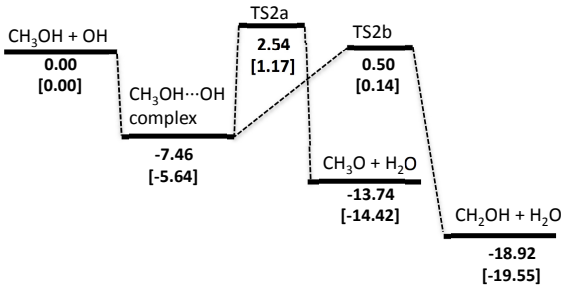

Fig. 2 Relative energies (in kcal/mol) of the stationary points calculated at the MPWB1K/6-31+G(d,p) level for the methanol plus OH hydrogen abstraction. Zero-point inclusive energies in brackets.

SBGH carried out master equation calculations based on electronic structure calculations of Ref. 1; in addition they used empirical one-dimensional Eckart barriers for their tunneling calculations with parameters derived from the observed rate constants, i.e. optimized towards the desired results. For instance, for reaction R2a they adopted an imaginary frequency of 2564 cm^{-1}, leading to a barrier which is too high and too thin. Our calculated imaginary frequency equals 1737 cm^{-1}, which is clearly a more realistic value. For hydrogen abstraction from methanol by atomic hydrogen one of us also found that the Eckart barrier led to an overestimation of the tunneling contribution when compared to a multi-dimensional tunneling method.[27] For instance at 100 K, the calculated values by SBGH and by us are 2.14×10^{-12} cm^3 $molecule^{-1}$ s^{-1} and 0.99×10^{-12} cm^3 $molecule^{-1}$ s^{-1}, respectively. In this context, the SBGH calculations can be regarded as an upper limit for the monomer mechanism at low temperatures. With the newly calculated potentials,tunneling probabilities and reaction dynamics models, the discrepancy between experimental and theoretical results does not disappear; in fact it is further enhanced, since the rate constants calculated in this study are smaller than those obtained by SBGH. We therefore abandoned this route in favor of a more promising alternative: investigating the reactivity of dimers.

Methanol dimer mechanism

In the low-temperature experiment (below 100 K) of Refs. 4 and 8, the reaction mixture is cooled by expansion with a carrier gas through a pulsed Laval nozzle. The reaction mixture consists of methanol and a hydroxyl radical precursor. The progress of the reaction is monitored by measuring the disappearance of these radicals. It is known, however, that such an expansion of a gas with molecules that can interact through hydrogen bonding[28,29] or other intermolecular forces[30,31] tends to produce not only monomers but also dimers and, depending on the structure and experimental conditions, larger clusters. This is also the case with methanol, which at low temperatures and under certain conditions, including experiments in supersonic Laval nozzles,[32] forms clusters,[33] and mainly dimers.[34] Because of the low collision rate of the beam, the resulting mixture of monomers and dimers (with the dimer having a binding energy of 6.1 kcal/mol), is not in chemical equilibrium, i.e., dimers formed during the expansion will tend to survive until they collide with hydroxyl radicals. Therefore the possible presence of dimers (and possibly larger clusters, which we will neglect henceforth) in the expanded gas should not be ignored.

Compared to monomeric methanol (M), the cross-section of the dimer (D) may be larger, thus being a preferred target for the hydroxyl radical. But more important is the fact that the dimer can dissociate, thus providing the required third body to stabilize the reaction complex. The probable outcome of a collision of the dimer with hydroxyl is that the hydroxyl moiety, because of its stronger binding, replaces a methanol molecule, and that the small amount of heat generated will be mostly carried off as kinetic energy by the replaced molecule, thus leaving a cool complex. In this case the reaction mechanism involves the following elementary steps:

$$(CH_3OH)_2 + OH \xrightarrow{k_{1,D}} C' + CH_3OH \qquad \text{(R1')}$$

$$C' \xrightarrow{k_{-1,D}} CH_3OH + OH \qquad \text{(R-1')}$$

$$C' \xrightarrow{k_{2a,D}} CH_2OH + H_2O \qquad \text{(R2a')}$$

$$C' \xrightarrow{k_{2b,D}} CH_3O + H_2O \qquad \text{(R2b')}$$

Since the opening of this new channel would provide a way out of the dilemma discussed above, an investigation of its quantitative effects is called for.

QCT calculations carried out for the association reaction (R1') yield an internal energy distribution function for the nascent complex (C') of Gaussian form (see Fig. 3). However, since this Gaussian enters the quantum mechanically forbidden region (below the zero-point energy of the complex), we have also employed unshifted but 10 times thinner Gaussian distributions. This procedure resembles the Gaussian binning method,[35] and avoids to a large extent zero-point energy leakage. The effect of this modification in the total thermal rate constant $k_D(T)$ is about a factor

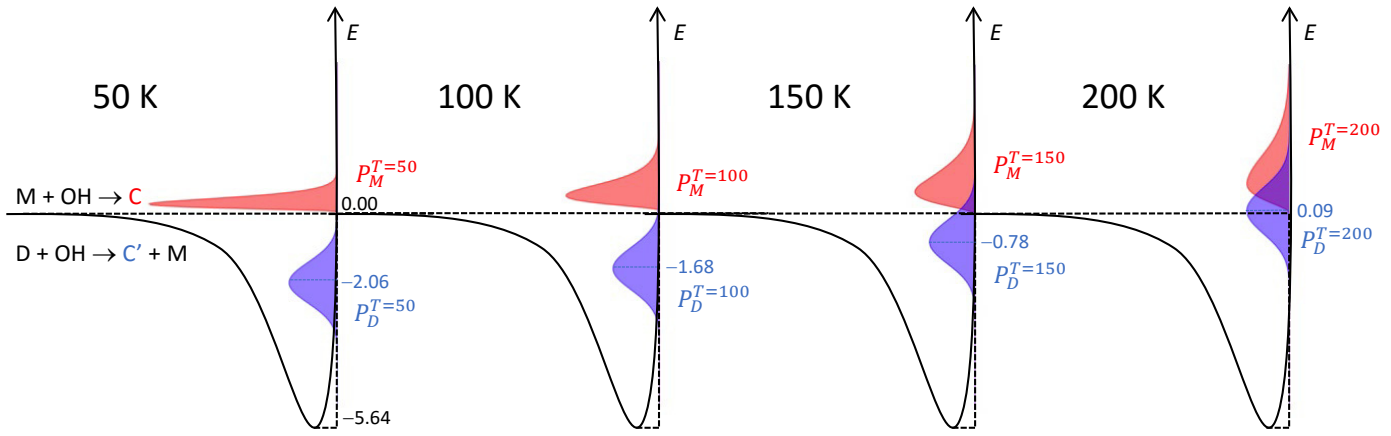

Fig. 3 Internal energy distributions of the nascent complexes in the monomer and dimer mechanisms. The blue numbers indicate the average internal energies of the complexes formed in the dimer mechanism (in kcal/mol and including ZPE).

of two. For instance, at $T = 50$ K with the original distribution $k_{\mathrm{D}}(T) = 1.82 \times 10^{-10}$ cm^3 molecule^{-1} s^{-1}, whereas the modified distribution leads to $k_{\mathrm{D}}(T) = 3.59 \times 10^{-10}$ cm^3 molecule^{-1} s^{-1}. Table 1 lists the average of the two values.

As expected, the D + OH association rate constant $k_{1,\mathrm{D}}$ is 2 to 3 times larger than the M + OH capture rate $k_{1,\mathrm{M}}$ (Table 1). Additionally, the QCT simulations show that two different mechanisms can take place upon capture in the D + OH reaction: (i) *Inelastic scattering*, where the dimer survives the collision with hydroxyl, and the only consequence of the interaction is an energy exchange; these capture trajectories are therefore considered unreactive; (ii) *Substitution*, where the hydroxyl replaces either of the methanol molecules in the dimer, which leads to the complex C'. This mechanism enhances the overall rate, as the resulting complexes are much cooler than those formed in the corresponding M + OH reaction. According to our QCT simulations, the *substitution* mechanism accounts for 72%, 69%, 68% and 68% of the total at $T = 50$, 100, 150 and 200 K, respectively. Representative movies of each mechanism are included in the SI. Apparently, the inelastic scattering mechanism is more favored in the reaction of hydroxyl with bulkier alcohols such as ethanol and 2-propanol, possibly because the methyl groups screen the hydroxyl group. That would explain that these alcohols display less reactivity towards OH at low temperatures.[36]

Figure 3 demonstrates that in D + OH collisions a significant amount of energy is carried off by the leaving monomer, leading to rovibrationally cold complexes. The nascent complexes (C') have average internal energies of −2.06, −1.68, −0.78 and 0.09 kcal/mol (with respect to the M + OH dissociation limit) for $T = 50$, 100, 150 and 200 K, respectively. For the lowest two temperatures the average internal energies are well below the dissociation energy, which means that an important fraction of these complexes will proceed to products before they can redissociate. This result indicates that the overall rate constant $k_{\mathrm{D}}(T)$ for the D + OH mechanism is greater than that of the M + OH mechanism, and close to the association rate constant $k_{1,\mathrm{D}}(T)$ (see Table 1).

Table 1 Association ($k_{1,\mathrm{M}}(T)$ and $k_{1,\mathrm{D}}(T)$) and total ($k_{\mathrm{M}}(T)$ and $k_{\mathrm{D}}(T)$) thermal rate constants for the reaction of methanol monomer (M) and methanol dimer (D) with the OH radical. The last column list the total rate constant for the hydrogen abstraction reaction obtained from eqn 2. All thermal rate constants in 10^{-12} cm^3 molecule^{-1} s^{-1}

T(K)	$k_{1,\mathrm{M}}(T)$	$k_{1,\mathrm{D}}(T)$	$k_{\mathrm{M}}(T)$	$k_{\mathrm{D}}(T)$	$k(T)$
50	278	499	1.67	271	41.8
100	233	489	0.99	248	26.3
150	213	446	0.90	205	0.98
200	174	412	0.80	114	0.80

Comparison with experiments

The main result of this study is that, under cold beam conditions, methanol dimers react much faster with hydroxyl radicals than methanol monomers. Whether this result has relevance for the observations reported in Refs. 4 and 8 depends on the presence or absence of dimers in the beams. This can only be established experimentally. If equilibrium conditions prevailed, the dimer fraction would vary from close to zero above 150 K to close to 100 % below 50 K for the calculated dimer binding energy of 6.1 kcal/mol. However, it has been found that Laval nozzles generate beams in which the actual concentration need not be the equilibrium concentration but may be smaller or larger depending on the conditions.[37] Presumably, the value is set inside the nozzle and remains virtually unchanged in the beam where there are few collisions. In the absence of specific information about the dimer fraction in the beam, we start our analysis from the observed rate constants and use our calculation scheme to calculate the dimer fraction required to reproduce these rate constants theoretically. Taking into account that the methanol concentration [Met] relates to the monomer [M] and dimer [D] concentrations by [Met] = [M] + 2[D], the total rate constant can be expressed as:

$$k(T) = k_{\mathrm{M}}(T)(1-2y) + k_{\mathrm{D}}(T)y, \qquad (2)$$

where y=[D]/[Met] is the unknown in the equation. Notice that the dimer fraction y is assumed to be constant for every tem-

perature, i.e., the dimer concentration depends linearly on the methanol concentration, which accounts for the linear dependence of the pseudo-first order experimental rates on methanol concentration.[4,8] This assumption is supported by a recent Laval-nozzle experiment with propane as the condensable gas, in which the average size of the clusters was found to be nearly independent of the propane concentration for low gas densities, an observation that is compatible with eqn 2.[38]

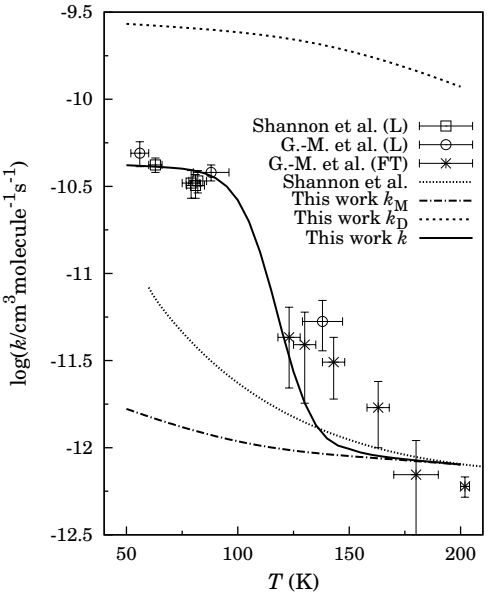

Fig. 4 Calculated and observed thermal rate constants plotted logarithmically against temperature. (L) and (FT) mean Laval and flow tube experiments, respectively.

The observed rate constants, displayed in Fig. 4, were obtained by a variety of methods and show considerable scattering. The calculated equilibrium rate constants (see SI) for the reaction

$2\mathrm{M} \rightleftharpoons \mathrm{D}$

indicate that at $T < 100$ K the dimer fraction strongly dominates ($2y_{\mathrm{eq}} \sim 1$) and that at $T > 150$ K, the dimer fraction is negligible ($2y_{\mathrm{eq}} \sim 0$), where $y_{\mathrm{eq}} = [\mathrm{D}]_{\mathrm{eq}}/[\mathrm{Met}]$ and $[\mathrm{D}]_{\mathrm{eq}}$ is the dimer concentration at equilibrium. Because of the scarcity of accurate data in the critical intermediate region (100-150 K), we cannot fit y reliably using this data. By contrast, the available rates at $T < 100$ K are accurate, and a good fit to the experiments is obtained when $2y \simeq 0.30$. Here we are assuming that the ratio $\alpha = y/y_{\mathrm{eq}}$ is temperature independent and equals that obtained at $T < 100$ K, namely 0.30. We can now express eqn 2 as a function a single and constant parameter α:

$$k(T) = k_{\mathrm{M}}(T)(1 - 2y_{\mathrm{eq}}\alpha) + k_{\mathrm{D}}(T)y_{\mathrm{eq}}\alpha, \qquad (3)$$

In Fig. 4, the choice of $\alpha = 0.30$ for all temperatures is represented by the solid curve, which yields a good fit to the experimental data from $T = 50$ to 200 K. It slightly underestimates the rates observed in the intermediate region; this may suggest that the dimer concentration could be closer to its equilibrium value, which would not be a surprise,[37] but cannot be firmly stated on the basis of the scattered data presently available. However, the significant point of this comparison is that it offers a concrete estimate of the dimer concentration in the Laval-nozzle beam at low temperatures, which can be tested experimentally.

Our estimate is supported by the observed very weak pressure effect. To show this, we computed the variation of the bimolecular rates with bath gas density for a density range of $0-17\times10^{16}$ molecule cm^3 at a temperature of 82 K. The theoretical result at this temperature was obtained via a linear interpolation between the 50 K and 100 K results. The rates obtained for the M + OH reaction show a slight increase with pressure (17% when $[N_2]$ changes from 0 to 17×10^{16} molecule cm^3), while the D + OH rates are very close to the capture limit and thus virtually independent of pressure. For the chosen value $\alpha = 0.30$ there is an almost perfect match with the observed rates (see the SI).

Moreover, the calculated branching ratios are in agreement with the observations and calculations of SBGH,[4] who predicted that at 70 K the dominant product is methoxy, whereas at room temperature the main product is hydroxymethyl.[3] Our results at $T = 50$, 100, 150 and 200 K yield 86, 67, 46 and 38% of methoxy radical formation, respectively. These results indicate that tunneling plays a role even at temperatures at which the reaction is controlled by the association reaction ($T < 100$ K) with a dominant contribution by the methanol dimer. In fact, most of the complexes formed from the methanol dimer have not enough energy to dissociate nor to proceed over the barrier, so tunneling decides which product dominates. Because tunneling is very sensitive to the width of the potential barrier, it is not surprising that the process with the highest imaginary frequency at the transition state (i.e. the narrowest potential) provides the dominant channel. As the temperature increases, overbarrier processes start to dominate for which the main product is the one whose formation is governed by the lowest barrier.

Conclusions

The present calculations show that dimerization greatly enhances the reactivity of methanol towards hydroxyl radicals at low temperature. This raises the question whether the recently observed increase in reactivity with decreasing temperature in Laval-nozzle beams is due to dimerization or formation of a hot collision complex with a lifetime long enough to allow reaction by proton tunneling. Our calculations indicate that both reaction channels contribute but that below a temperature of 100 K the dimer channel dominates. Specifically, they predict that at those temperatures, the concentration of dimers in the beam used in the experiments needs to be about 30 % of the equilibrium concentration in order to account for the observed rates, a conclusion that can be tested experimentally, since the dimer has been identified spectroscopically. If the test result is positive, the problem of the high reactivity at low temperatures is basically solved; if it is negative the problem remains open, since the available calculations based exclusively on the monomer channel lead to rates at least an order of magnitude lower than observed.

Our calculations have also astrophysical relevance since the reaction has been proposed[4] as a source of methoxy radicals recently detected in interstellar space, where the dimerization channel should not be available. This leads to the general conclusion

that for reactions that are enhanced by the formation of clusters, including dimers, data obtained from cold-beam experiments can be applied to interstellar chemistry only if they can be corrected for the presence of clusters.

Acknowledgements

A. F. R. and E. M. N. acknowledge funding from Ministerio de Economia y Competitividad of Spain (Research Grant No CTQ2014-58617-R). E. M. N. acknowledges financial support from Xunta de Galicia (Research Grant No GRC2014/032). The corresponding authors thank D. Shalashilin for helpful discussions and his invitation to the University of Leeds. The authors also thank D. E. Heard and J. M. C. Plane of the University of Leeds for helful comments. We thank the Centro de Supercomputación de Galicia (CESGA) for computational facilities.

References

1 S. Xu and M. C. Lin, *Proc. Combust. Inst.*, 2007, **31**, 159–166.

2 W. P. Hess and F. P. Tully, *J. Phys. Chem.*, 1989, **93**, 1944–1947.

3 T. J. Dillon, D. Holscher, V. Sivakumaran, A. Horowitz and J. N. A. Crowley, *Phys. Chem. Chem. Phys.*, 2005, **7**, 349–355.

4 R. J. Shannon, M. A. Blitz, A. Goddard and D. E. Heard, *Nature Chem.*, 2013, **5**, 745–749.

5 E. Herbst, *J. Phys. Chem. A*, 2005, **109**, 4017–4029.

6 J. Cernicharo, N. Marcelino, E. Roueff, M. Gerin, A. Jiménez-Escobar and G. M. M. noz Caro, *Astrophys. J. Lett.*, 2012, **759**, L43.

7 K. Acharyya, R. L. Herbst, E. anf Caravan, R. J. Shannon, M. A. Blitz and D. E. Heard, *Mol. Phys.*, 2015, **113**, 2243–2254.

8 J. C. Gómez-Martín, R. L. Caravan, M. A. Blitz, D. E. Heard and J. M. C. Plane, *J. Phys. Chem. A*, 2014, **118**, 2693–2701.

9 W. J. Hehre, R. Ditchfield and J. A. Pople, *J. Chem. Phys.*, 1972, **56**, 2257–2261.

10 Y. Zhao, B. J. Lynch and D. G. Truhlar, *J. Phys. Chem A*, 2004, **108**, 6908–6918.

11 Y. Zhao, N. E. Schultz and D. G. Truhlar, *J. Chem. Theory Comput.*, 2006, **2**, 364–382.

12 G. R. Shelton, D. A. Hrovat and W. T. Borden, *J. Am. Chem. Soc.*, 2007, **129**, 164–168.

13 R. Meana-Pañeda and A. Fernández-Ramos, *J. Am. Chem. Soc.*, 2012, **134**, 346–354; (E) **2012**, *134*, 7193.

14 I. M. Alecu, J. Zheng, Y. Zhao and D. G. Truhlar, *J. Chem. Theory Comput.*, 2010, **6**, 2872–2887.

15 Y.-P. Liu, G. C. Lynch, T. N. Truong, D.-h. Lu and D. G. Truhlar, *J. Am. Chem. Soc.*, 1993, **115**, 2408–2415.

16 A. Fernández-Ramos, A. Ellingson, B. C. Garrett and D. G. Truhlar, *Rev. Comput. Chem.*, 2007, **23**, 125.

17 J. W. Davies, N. J. B. Green and M. J. Pilling, *Chem. Phys. Lett.*, 1986, **126**, 373–379.

18 A. Fernández-Ramos, J. A. Miller, S. J. Klippenstein and D. G. Truhlar, *Chem. Rev.*, 2006, **106**, 4518.

19 D. R. Glowacki, C.-H. Lian, C. Morley and M. J. Pilling, *J. Phys. Chem. A*, 2012, **116**, 9545–9560.

20 M. J. T. Jordan, S. C. Smith and R. G. Gilbert, *J. Chem Phys.*, 1991, **95**, 8685–8694.

21 D. T. Gillespie, *J. Comput. Chem.*, 1976, **22**, 403–434.

22 R. L. Rowley, C. M. Tracy and T. A. Pakkanen, *J. Chem. Phys.*, 2006, **125**, 154302.

23 M. J. Frisch, G. W. Trucks, H. B. Schlegel, G. E. Scuseria, M. A. Robb, J. R. Cheeseman, G.Scalmani, V. Barone, B. Mennucci, G. A. Petersson, H. Nakatsuji, M. Caricato, X. Li, H. P. Hratchian, A. F. Izmaylov, J. Bloino, G. Zheng, J. L. Sonnenberg, M. Hada, M. Ehara, K. Toyota, R. Fukuda, J. Hasegawa, M. Ishida, T. Nakajima, Y. Honda, O. Kitao, H. Nakai, T. Vreven, J. A. Montgomery Jr., J. E. Peralta, F. Ogliaro, M. Bearpark, J. J. Heyd, E. Brothers, K. N. Kudin, V. N. Staroverov, R. Kobayashi, J. Normand, K. Raghavachari, A. Rendell, J. C. Burant, S. S. Iyengar, J. Tomasi, M. Cossi, N. Rega, J. M. Millam, M. Klene, J. E. Knox, J. B. Cross, V. Bakken, C. Adamo, J. Jaramillo, R. Gomperts, R. E. Stratmann, O. Yazyev, A. J. Austin, R. Cammi, C. Pomelli, J. W. Ochterski, R. L. Martin, K. Morokuma, V. G. Zakrzewski, G. A. Voth, P. Salvador, J. J. Dannenberg, S. Dapprich, A. D. Daniels, O. Farkas, J. B. Foresman, J. V. Ortiz, J. Cioslowski and D. J. Fox, Gaussian09, Gaussian, Inc., Wallingford CT, (2009).

24 W. L. Hase, R. J. Duchovic, X. Hu, A. Komornicki, K. F. Lim, D.-H. Lu, G. H. Peslherbe, K. N. Swamy, S. R. Vande Linde, A. Varandas, H. Wang and R. J. Wolf, *Quantum Chemistry Programs Exchange (QCPE) Bulletin*, 1996, **16**, 671.

25 J. C. Corchado, Y.-Y. Chuang, P. L. Fast, W.-P. Hu, Y.-P. Liu, G. C. Lynch, K. A. Nguyen, C. F. Jackels, A. Fernández-Ramos, B. A. Ellingson, B. J. Lynch, J. Zheng, V. S. Melissas, J. Villa, I. Rossi, E. L. Coitiño, J. Pu, T. V. Albu, R. Steckler, B. C. Garrett, A. D. Isaacson and D. G. Truhlar, POLYRATE−version 9.7, University of Minnesota, Minneapolis, (2007).

26 F. J. Hernandez, J. T. Brice, C. M. Leavitt, G. A. Pino and G. E. Douberly, *J. Phys. Chem. A*, 2015, **119**, 8125–8132.

27 R. Meana-Pañeda, D. G. Truhlar and A. Fernández-Ramos, *J. Chem. Phys.*, 2011, **134**, 0943202.

28 O. Birer and M. Havenith, *Annu. Rev. Phys. Chem.*, 2009, **60**, 263–275.

29 J. Bourgalais, V. Roussel, M. Capron, A. Benidar, A. W. Jasper, S. J. Klippenstein, L. Biennier and S. D. Le Picard, *Phys. Rev. Lett.*, 2016, **116**, 113401.

30 S. Hamon, S. D. Le Picard, A. Canosa, B. R. Rowe and I. W. M. Smith, *J. Chem Phys.*, 2000, **112**, 4506–4516.

31 H. Sabbath, L. Biennier, S. J. Klippenstein, I. R. Sims and B. R. Rowe, *J. Phys. Chem. Lett.*, 2010, **1**, 2962–2967.

32 H. Laksmono, S. Tanimura, H. C. Allen, G. Wilenski, M. S. Zahniser, J. H. Shorter, D. D. Nelson, J. B. McManus and B. E. Wyslouzil, *Phys. Chem. Chem. Phys.*, 2011, **13**, 5855–5871.

33 U. Bux, X. J. Gu, C. Lauenstein and A. Rudolph, *J. Chem. Phys.*, 1990, **92**, 6017–6029.

34 F. Kollipost, A. Andersen, D. W. Mahler, J. Heimdal, M. Heger, M. A. Suhm and R. W. Larsen, *J. Chem. Phys.*, 2014, **141**, 174314.

35 L. Bonnet and J. C. Rayez, *Chem. Phys. Lett.*, 1997, **277**, 183–190.

36 R. L. Caravan, R. J. Shannon, T. Lewis, M. A. Blitz and D. E. Heard, *J. Phys. Chem. A*, 2015, **119**, 7130–7137.

37 S. Tanimura, B. A. Wyslouzyl and G. Willemski, *J. Chem. Phys.*, 2010, **132**, 144301.

38 J. J. Ferreiro, T. E. Gartmann, B. Schläppi and R. Signorell, *Z. Phys. Chem.*, 2015, **229**, 1765–1780.